



Solar light-driven photocatalytic degradation of Anthraquinone dye-contaminated water by engineered Ag@TiO₂ core-shell nanoparticles

Ankita Khanna, Vidya Shetty K*

Department of Chemical Engineering, National Institute of Technology Karnataka, Surathkal, Mangalore 575 025, India
Tel. +91 824 2474000 - 3606; Fax: +91 824 2474033; email: vidyaks68@yahoo.com

Received 24 August 2013; Accepted 17 January 2014

ABSTRACT

The Ag core-TiO₂ shell (Ag@TiO₂) nanoparticles were synthesized by one-pot synthesis method followed by calcination and characterized using X-ray diffraction and transmission electron microscopy. The Ag@TiO₂ core-shell-structured nanocatalyst was evaluated for its photocatalytic activity towards the degradation of Acid Blue-129 (AB-129), an Anthraquinone dye under solar light irradiations. The nanoparticles were engineered for efficient photocatalytic degradation of AB-129 by varying the parameters such as catalyst composition, calcination temperature, and calcination time. The catalyst composition with Ag to Ti molar ratio of 1:1.7, calcination temperature of 450°C, and time of 3 h were found to be the optimum for the efficient photocatalytic degradation of AB-129. The efficacy of Ag@TiO₂ was compared with commercial TiO₂, synthesized nano-TiO₂, and Ag-doped TiO₂ for the photocatalytic degradation of AB-129 and enhanced dye degradation was obtained with Ag@TiO₂. This enhanced activity of Ag@TiO₂ may be attributed to the trapping of conduction band electrons in Ag core and subsequent discharge on supply of air. Solar photocatalytic degradation of AB-129 dye using Ag@TiO₂ followed Langmuir-Hinshelwood kinetics. Ag@TiO₂ can be exploited as an efficient catalyst for the degradation of dye and textile industry wastewater.

Keywords: Core-shell nanoparticles; Calcination; Dyes; Photocatalysis; Solar light irradiation

1. Introduction

Industrial dyestuffs including textile dyes are the primary source of discharge of dyes into the environment. More than 10,000 dyes with an annual production over 7×10^5 MT are commercially available worldwide [1]. Due to the complex aromatic structure and stability, dyes are categorized as environmentally hazardous materials and conventional biological treatment methods are ineffective for degradation of these dyes [2]. Adsorption by activated carbon and

enhanced coagulation are commonly employed for dye removal from wastewater [3] but, however, further treatment is necessary because these methods transfer dyes from one form to other form. Recently, photocatalysis has gained considerable attention due to its compliance with green chemistry concept. This method leads to complete mineralization of organic compounds to H₂O and CO₂. Moreover, photocatalysis does not require expensive oxidants (atmospheric oxygen is used as oxidant) and can be carried out at mild temperature and pressure. Photocatalysis process is receiving much interest because of its low cost

*Corresponding author.

when sunlight is used as the source of irradiation [4]. The solar heterogeneous photocatalytic degradation process generally utilizes the near-UV part of the solar spectrum (wavelength shorter than 380 nm) [5], to photoexcite a semiconductor catalyst in the presence of atmospheric oxygen which is easily involved as an oxidant to yield the oxidizing species (O_2^- and OH radicals), which can cause photodegradation [6]. The application of solar-powered photocatalysis to treat textile industrial wastewater holds promise for regions receiving strong sunlight throughout the year, such as India which receives an adequate amount of solar radiation for almost 10 months a year [7]. Since, TiO_2 can only use a relatively small part of solar light which consists of 4–5% of UV radiations [8] and hence photocatalysis using TiO_2 as a catalyst is not effective under solar irradiation. So, the use of photocatalysts which can be excited by both visible and UV light of solar radiation can essentially increase the efficiency of photocatalytic process. Noble metals such as Ag, Au, Pt, and Pd deposited on a TiO_2 surface could enhance the photocatalytic efficiencies because they act as an electron trap promoting interfacial charge transfer processes in the composite systems [9,10]. But this type of catalyst structure, though effective, results in exposing noble metal to reactants and the surrounding medium [11]. Metals on the surface of the semiconductor will be easily corroded and dissolved. An efficient way to overcome these drawbacks is to exploit a core-shell-type structure in which the noble metal particles are introduced as cores and the semiconductor dioxide such as TiO_2 as shells [12–15]. Hirakawa and Kamat [16] found that $Ag@TiO_2$ core-shell nanoparticles exhibit strong absorption of light in the visible range and photoexcitation of TiO_2 shell which results in generation of electrons and holes. The electrons get accumulated in Ag core of $Ag@TiO_2$ nanoparticle until the Fermi level equilibrium is achieved and the electrons get discharged when an electron acceptor such as O_2 is introduced into the system [16]. Since dissolved oxygen is a good acceptor of electrons, some of the electrons can move to TiO_2 shell which further get reduced to superoxide anion (O_2^-). The holes can either react with hydroxyl anion (OH^-) or H_2O to produce hydroxyl radical ($\cdot OH$). These radicals ($\cdot OH$, O_2^-) are powerful oxidizing agents and are reported to be responsible for the photocatalysis of dyes [17]. The detailed mechanism of $Ag@TiO_2$ nanoparticle is shown in Fig. 1.

Anthraquinone dyes are the second most important class of commercial dyes after azo dye and are characterized by their brightness and good fastness and they gain wide applications in textile industry. On the other hand, serious environmental problems are also associated with this class of dyes. So, in the

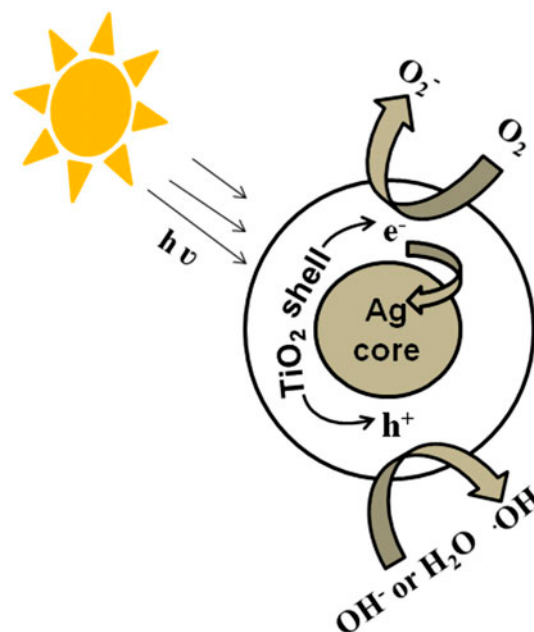


Fig. 1. The possible mechanism of photocatalysis by $Ag@TiO_2$ nanoparticles.

present study, $Ag@TiO_2$ nanoparticles have been synthesized on the basis of one-pot synthesis route followed by Hirakawa and Kamat [11]. It is necessary to engineer the nanoparticles for better photocatalytic activity. It can be done by varying the composition of the nanoparticle, calcination temperature, and calcination time. The current investigation focuses on engineering $Ag@TiO_2$ nanoparticles by optimization of Ag to Ti ratio, calcinations temperature and time for enhancement in solar photocatalytic activity and hence its utilization in treatment of dye-contaminated wastewater is explored. The photocatalytic activity of these nanoparticles is then compared with P-25, synthesized TiO_2 , and Ag-doped TiO_2 for the photocatalytic degradation of Acid Blue-129 (AB-129), an Anthraquinone dye under solar light irradiation. To the best of our knowledge, this is a first report on the use of $Ag@TiO_2$ core-shell-structured nanoparticles for the photocatalytic degradation of an Anthraquinone dye under solar light irradiation.

2. Experimental section

2.1. Materials

AB-129 dye was purchased from Sigma-Aldrich and was used without further purification (Table 1). Titanium-(triethanolaminate) isopropoxide ($N((CH_2)_2O)_3TiOCH(CH_3)_2$) (TTEAIP) and titanium tetraisopropoxide (TTIP) were purchased from Sigma-Aldrich, 2-propanol (GR grade), dimethyl formamide

(DMF), glycine, acetic acid, nitric acid (HNO₃), ethanol, and silver nitrate (AgNO₃) were purchased from Merck and used as received. Degussa P-25 was obtained as a gift pack from Evonik Degussa India Pvt. Ltd. It consists of 75% anatase and 25% rutile with a specific BET surface area of 50 m²/g and primary particle size of 20 nm. Care should be taken to handle toxic solvents such as DMF and hygroscopic materials such as TTEAIP. Sodium hydroxide (NaOH) and sulfuric acid (H₂SO₄) were purchased from Merck for adjustment of pH of the dye solutions. Distilled water was used in all the experiments.

2.2. Preparation of Ag@TiO₂, TiO₂, and Ag-doped TiO₂

For the synthesis of Ag@TiO₂ core-shell-structured nanoparticles, one-pot synthesis method of hydrolysis of TTEAIP and the reduction of metal ions in DMF, as has been followed by Hirakawa and Kamat [11], were used, by varying Ag to Ti ratios in the reaction mixture. About 8.3 mM of TTEAIP solution was prepared in 2-propanol and 15 mM of AgNO₃ solution was prepared. About 2 mL of 15 mM AgNO₃ solution was mixed with 18 mL of TTEAIP solution. The concentration of Ag⁺ and TTEAIP in the reaction mixture was 1 and 5 mM, respectively. The concentration of AgNO₃ in the mixture was kept constant at 1 mM and TTEAIP concentration in the reaction mixture was varied as 5, 3.1, 2.2, 1.7, and 0.8 mM, respectively, by suitably varying the volume of 8.3 mM of TTEAIP solution added. The solution was stirred first for 15 min at room temperature and 10 mL of DMF was then added into TTEAIP-Ag solution. The mixture was heated with reflux and continued stirring. With continued heating of the solution, the color slowly changed from colorless to light brown. After 90 min, the color of the suspension turned to dark brown. At this point, the

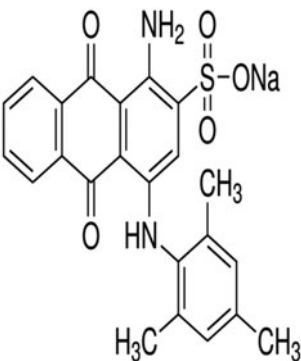
heating was stopped and the suspension was stirred until it cooled to room temperature. The cluster suspension of Ag@TiO₂ was centrifuged and resuspended in ethanol solution. The procedure was repeated at least thrice to minimize the content of water and DMF in the suspension. After repeated ethanol washing and centrifugation, the particles were dried in a hot air oven at 100°C for 2 h. The particles were then calcined at a specific required temperature in the range of 150 to 550°C in a muffle furnace for a calcination time period of 3 h. To study the effect of calcinations time, the calcination was carried out for a different time period of 1–5 h. After calcination, the particles were stored as suspension in ethanol until its use. Prior to use, the particles were separated from ethanol by centrifugation and dried.

For preparation of sol-gel synthesized TiO₂ (SGTiO₂), procedure followed by Rupa et al. [18], for combustion synthesized TiO₂ (CSTiO₂), procedure followed by Nagaveni et al. [19], for sol-gel synthesized TiO₂ with doped silver (Ag doped-SGTiO₂), procedure followed by Zhang et al. [20], for combustion synthesized TiO₂ with Ag doping by liquid impregnation (Ag doped (LI)-CSTiO₂), procedure reported by Sahoo and Gupta [21] and Behnajady et al. [22] and for combustion synthesized TiO₂ with Ag doping by photodeposition (Ag doped (PD)-CSTiO₂), procedure given by Behnajady et al. [22] were followed. For Ag-doped TiO₂ catalyst preparation, Ag to Ti molar composition ratio of 1:1.7 was used. All TiO₂ and Ag-doped TiO₂ nanoparticles prepared were calcined at 450°C for 3 h.

2.3. Characterization of Ag@TiO₂ nanoparticles

The X-ray diffraction (XRD) of Ag@TiO₂ core-shell structured nanoparticles prepared with different Ag to Ti molar composition ratios and after calcination at

Table 1
Structure and characteristic of AB-129 dye

Structure	Formula	Molecular weight (g/mol)	λ_{\max} (nm)
	C ₂₃ H ₂₁ N ₂ NaO ₅ S	460.48	630

450 °C for 3 h were done using JEOL X-ray Diffractometer, which helped in the determination of crystal structure and crystallite size of Ag@TiO₂ nanoparticles. The average crystallite size was found using the Scherrer's equation [23].

Transmission electron microscopy (TEM) analysis of the Ag@TiO₂ was done using a JEOL-JEM-2100 F microscope as illustrated by Khanna and Shetty [23].

2.4. Experimentation

The photocatalytic reactor is a 250-mL beaker made of borosilicate glass equipped with a magnetic stirrer. Batch photocatalytic degradation experiments were performed using Ag@TiO₂ core-shell-structured nanoparticles as the photocatalyst, to study the effect of catalyst calcination temperature and time on photocatalytic degradation of AB-129 under solar light irradiation. Experiments were conducted in an open terrace between 11.00 am and 2.00 pm on a sunny day. Solar light intensity was measured using UV intensity meter (UV-340A, Lutron) and visible light meter (KM-LUX-100K) for UV and visible light intensities. Also temperature of reaction mixture was measured and was found to be 32 ± 2 °C for the entire irradiation period of 3 h. Dissolved oxygen in the reaction mixture transferred from atmosphere, itself acted as an oxidant. In all the experiments, 100 mL dye solution in water with the required concentration of dye (10 mg/L) containing appropriate quantity of the photocatalyst was used. Initial pH of the solution was adjusted to a required value by adding 0.01 N H₂SO₄ and by measuring the pH with a pH meter (Equip-Tronics model no. EQ-610). Aqueous dye solutions were stirred magnetically. Aliquots of the samples were withdrawn at regular time intervals and centrifuged at 10,000 rpm for 5 min to separate the catalyst. The absorbance of the solution at 630 nm was measured by a UV-vis spectrophotometer (Hitachi model no. U-2000) and corresponding dye concentration in the solution was measured. The percentage of degradation was calculated from Eq. (1):

$$\text{Degradation (\%)} = (C_0 - C)/C_0 \times 100 \quad (1)$$

where C_0 is the initial dye concentration and C is the dye concentration in the reactor at any time.

Similar experiments were performed with different photocatalysts such as the commercially available Degussa P-25 catalyst, TiO₂ (SGTiO₂), CSTiO₂, Ag-doped SGTiO₂, Ag-doped (LI)-CSTiO₂, and Ag-doped (PD)-CSTiO₂ photocatalysts with dissolved

oxygen as the oxidant and the photocatalytic activity of these nanoparticles were compared in terms of photocatalytic degradation of AB-129, with those of Ag@TiO₂ core-shell-structured nanoparticles under solar light irradiation. The total organic carbon (TOC) was analyzed using TOC analyzer (TOC-V CSN, Shimadzu) and analysis of chemical oxygen demand (COD) was carried out as per the standard method for COD analysis [24].

3. Results and discussion

3.1. Engineering Ag@TiO₂ by optimization of catalyst composition, calcination temperature, and calcination time for enhancement in solar photocatalytic activity and degradation of AB-129

It is necessary to engineer the nanoparticles for better photocatalytic activity. It can be done by varying the composition of the nanoparticle, calcination temperature and calcination time. Ag@TiO₂ nanoparticles can be engineered by optimization of Ag to Ti molar ratio, calcinations temperature and time for enhancement of their solar photocatalytic activity. Molar ratio of Ag to TiO₂ may play an important role in the structure of the catalyst. Size of the core and shell of Ag@TiO₂ depends on the molar ratio of Ag to Ti [25], which in turn may affect the photocatalytic activity. It is well known that calcination temperature is an important factor that probably influences the crystallinity, morphology, and surface area of TiO₂, which can clearly affect the photocatalytic activity [26,27]. Crystallization plays a very important role in the photocatalytic activity of TiO₂. Enhancing calcination temperature improves the crystallization of TiO₂ which helps in the improvement of photocatalytic activity of TiO₂ [28,29]. A better crystallization means the decrease of crystal defects, which are the recombination centers of photo-induced charge carriers [30–34]. Thermal treatment helps in the phase transformation. Phase transformation of TiO₂ depends on the calcination temperature and composition [35]. Calcination temperature and time affect the crystalline nature and size of the catalyst and hence the catalytic characteristics are varied. To study the effect of calcination temperature of the catalyst, the degradation of AB-129 dye at initial concentration of 10 mg/L in aqueous solution with initial pH 3 was studied with the Ag@TiO₂ catalyst synthesized with different Ag to Ti molar ratios (1:5, 1:3.1, 1:2.2, 1:1.7, and 1:0.8) and calcined at temperatures ranging from 150 to 550 °C for calcination time of 3 h. Catalyst loading of 100 mg/L has been used in all the experiments. It was observed that as the calcination temperature increased, the percentage degradation of

AB-129 has increased. Figs. 2–6 show the time course variation of photocatalytic degradation of the AB-129 dye with Ag@TiO₂ catalyst prepared with different Ag to Ti molar ratio of 1:5, 1:3.1, 1:2.2, 1:1.7, and 1:0.8, respectively, under solar light irradiation. Effects of cat-

alyst calcination temperature on the photocatalytic degradation by Ag@TiO₂ catalyst prepared with different Ag to Ti molar ratio are shown in Figs. 2–6.

It can be seen from Figs. 2–6 that percentage degradation with noncalcined Ag@TiO₂ catalyst with

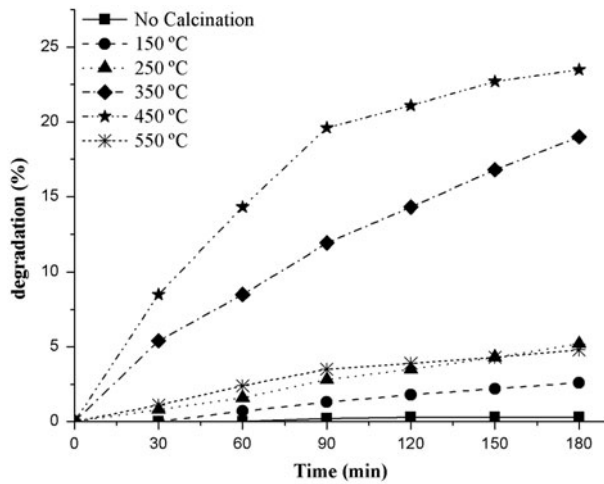


Fig. 2. Effect of calcination temperature on time course variation of solar photocatalytic degradation of AB-129 dye by Ag@TiO₂. Ag to Ti molar ratio = 1:5; calcination time = 3 h; pH 3; catalyst loading = 100 mg/L; C₀ = 10 mg/L; average UV and visible light intensities of solar light are 3.63 mW/cm² and 1,218 × 10² lux, respectively, from 11 am to 2 pm.

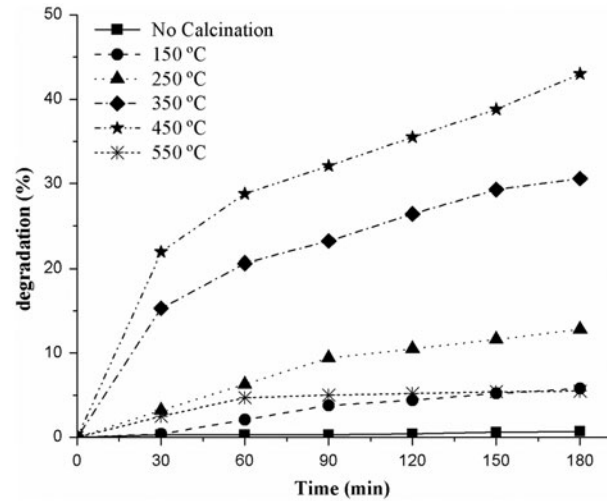


Fig. 4. Effect of calcination temperature on time course variation of solar photocatalytic degradation of AB-129 dye by Ag@TiO₂. Ag to Ti molar ratio = 1:2.2; calcination time = 3 h; pH 3; catalyst loading = 100 mg/L; C₀ = 10 mg/L; average UV and visible light intensity of solar light are 3.66 mW/cm² and 1,225 × 10² lux, respectively, from 11 am to 2 pm.

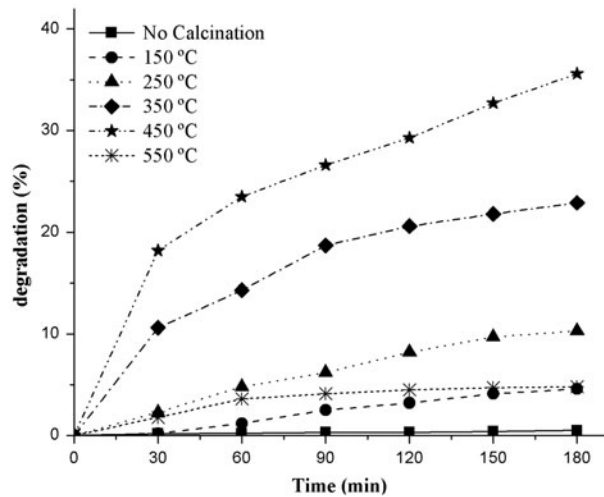


Fig. 3. Effect of calcination temperature on time course variation of solar photocatalytic degradation of AB-129 dye by Ag@TiO₂. Ag to Ti molar ratio = 1:3.1; calcination time = 3 h; pH 3; catalyst loading = 100 mg/L; C₀ = 10 mg/L; average UV and visible light intensity of solar light are 3.59 mW/cm² and 1,188 × 10² lux, respectively, from 11 am to 2 pm.

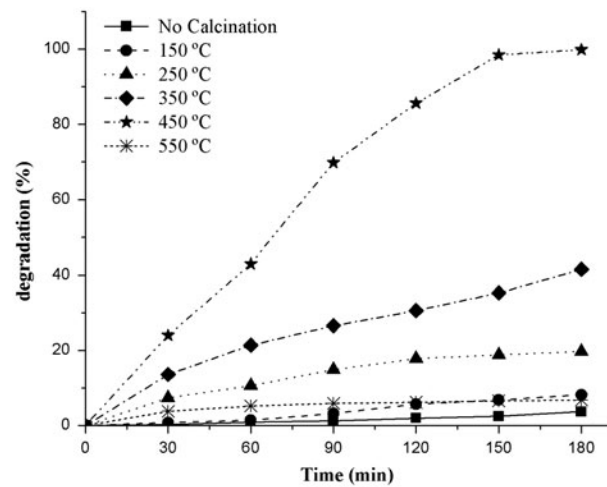


Fig. 5. Effect of calcination temperature on time course variation of solar photocatalytic degradation of AB-129 dye by Ag@TiO₂. Ag to Ti molar ratio = 1:1.7; calcination time = 3 h; pH 3; catalyst loading = 100 mg/L; C₀ = 10 mg/L; average UV and visible light intensity of solar light are 3.56 mW/cm² and 1,175 × 10² lux, respectively, from 11 am to 2 pm.

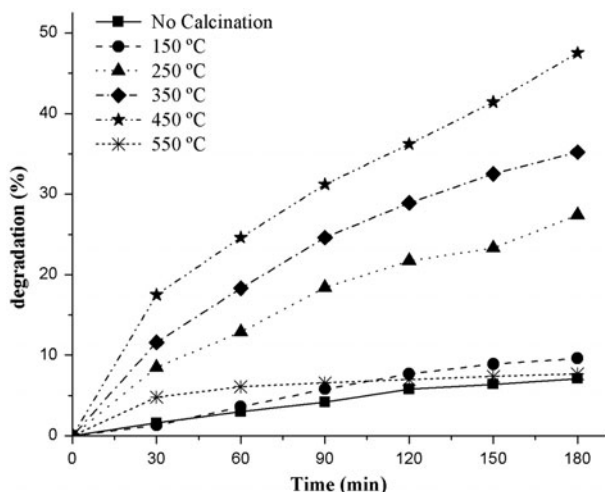


Fig. 6. Effect of calcination temperature on time course variation of solar photocatalytic degradation of AB-129 dye by Ag@TiO₂. Ag to Ti molar ratio = 1:0.8; calcination time = 3 h; pH 3; catalyst loading = 100 mg/L; C₀ = 10 mg/L; average UV and visible light intensity of solar light are 3.6 mW/cm² and 1,205 × 10² lux, respectively, from 11 am to 2 pm.

Ag to Ti molar ratios of 1:5, 1:3.1, 1:2.2, 1:1.7, and 1:0.8 is only 0.3, 0.4, 0.6, 2.46, and 6.4%, respectively, and are lesser than those obtained with the catalysts calcined at 150 °C. As the calcination temperature was increased from 150 to 450 °C, the degradation after 150 min of irradiation time has increased from 2.2 to 22.7% (with 1:5 M ratio), 4.1 to 32.7% (with 1:3.1 M ratio), 5.2 to 38.8% (with 1:2.2 M ratio), 6.8 to 98.5% (with 1:1.7 M ratio), and 8.9 to 41.4% (with 1:0.8 M ratio), but further increase in calcination temperature to 550 °C has decreased the degradation to only around 4.3% for 1:5, 4.7% for 1:3.1, 5.4% for 1:2.2, 6.6% for 1:1.7, and 7.4% for 1:0.8 Ag to Ti molar composition ratios. The highest degradation of AB-129 was observed with the catalysts (at all Ag to Ti molar composition ratios) calcined at calcination temperature of 450 °C. Increase in degradation with calcination temperature was attributed to the formation of crystalline phase of TiO₂, which increases with increasing calcination temperature, as reported by other researchers during degradation of acid red B dye [36] with Er³⁺: YAlO₃/ZnO–TiO₂ composite under sunlight. Increase in calcination temperature improves the crystallization and hence increases the activity of catalyst. TiO₂ has three crystalline phases: anatase, rutile, and brookite, among which anatase is more reactive than rutile and reported to be responsible for the photocatalysis. It is reported that as calcination temperature increases, the content of anatase phase increases but further increase in calcination temperature leads to change from ana-

tase to rutile phase and content of rutile increases as the temperature is increased [22,36,37].

In the present study, with nanoparticles calcined at 550 °C decreased, degradation was observed, which may be due to phase conversion from anatase to rutile phase. TG-DTA analysis of the synthesized nanoparticles with Ag to Ti ratio of 1:1.7 presented by Khanna and Shetty [23] showed a releasing peak at around 514 °C indicating the possible phase conversion of TiO₂ from anatase to rutile which supports the decrease in photocatalytic degradation with nanoparticles calcined at 550 °C. Similar observation was also made by Zhang et al. [38]. It is widely accepted that the anatase phase of titania is a relatively ideal photocatalytic material among its three crystalline phases [37]. It is also reported by other researchers [19,39,40] that TiO₂ containing only anatase phase showed better photocatalytic activity as compared to the commercial Degussa P-25 catalyst which consist of 75% anatase and 25% rutile phase. It is observed that as calcination temperature increases, photocatalytic activity increases, but further increase in calcination temperature leads to decrease in activity due to rutile phase formation. Decreased activity with nanoparticles calcined at 550 °C may also be due to the increase in silver content. It has also been observed that after calcination at 550 °C, the Ag@TiO₂ nanoparticles turned to gray lustrous surface, characteristic of Ag, instead of the blackish brown film of TiO₂ on the surface as was found in the catalyst after calcination at other temperatures. It was found that for catalysts prepared with all Ag to Ti molar ratios, as the calcination temperature was increased, degradation increased, but further increase in the calcination temperature to above 450 °C decreased the degradation. Hence, highest degradation was found at 450 °C.

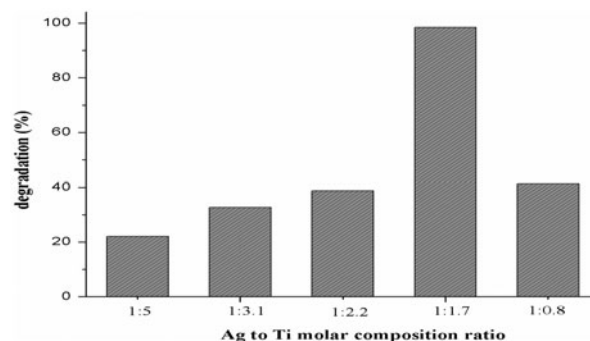


Fig. 7. Effect of Ag to Ti molar composition ratio on percentage degradation of AB-129 dye by Ag@TiO₂ nanoparticles calcined at 450 °C. Conditions: pH 3; catalyst loading = 100 mg/L; C₀ = 10 mg/L; irradiation time = 150 min.

Optimization of composition plays a very important role in the structure and morphology of the catalyst. Angkaew and Limsuwan [25] studied the effect of Ti to Ag molar ratio on two-step synthesized Ag@TiO₂ nanoparticles. They reported that at low concentration of TTIP as a precursor salt for Ti, TiO₂ can be effectively formulated on Ag nanoparticles which lead to the formation of core-shell structure, but higher concentration lead to formation of core-shell particles with larger shell thickness. However, in their studies, too high concentration of TTIP lead to the composite structure with Ag nanoparticles embedded in TiO₂ matrix. According to them, the effect of Ag-Ti mole ratio on the morphology of

nanoparticles can be explained in terms of the available nucleation sites and growth of titania particles on the pre-existing surface of silver nanoparticles. Since it was found that molar ratio is an important parameter in controlling the morphology of the resulting Ag@TiO₂ nanoparticles, so optimization of Ag to Ti molar ratio was carried out in the present study by varying the concentration of TTEAIP and AgNO₃ in the synthesis mixture for the formation of Ag core and TiO₂ shell.

Fig. 7 shows the effect of Ag:Ti molar ratio on percentage degradation (after 150 min of irradiation) of the dye by the nanoparticles calcined at 450°C.

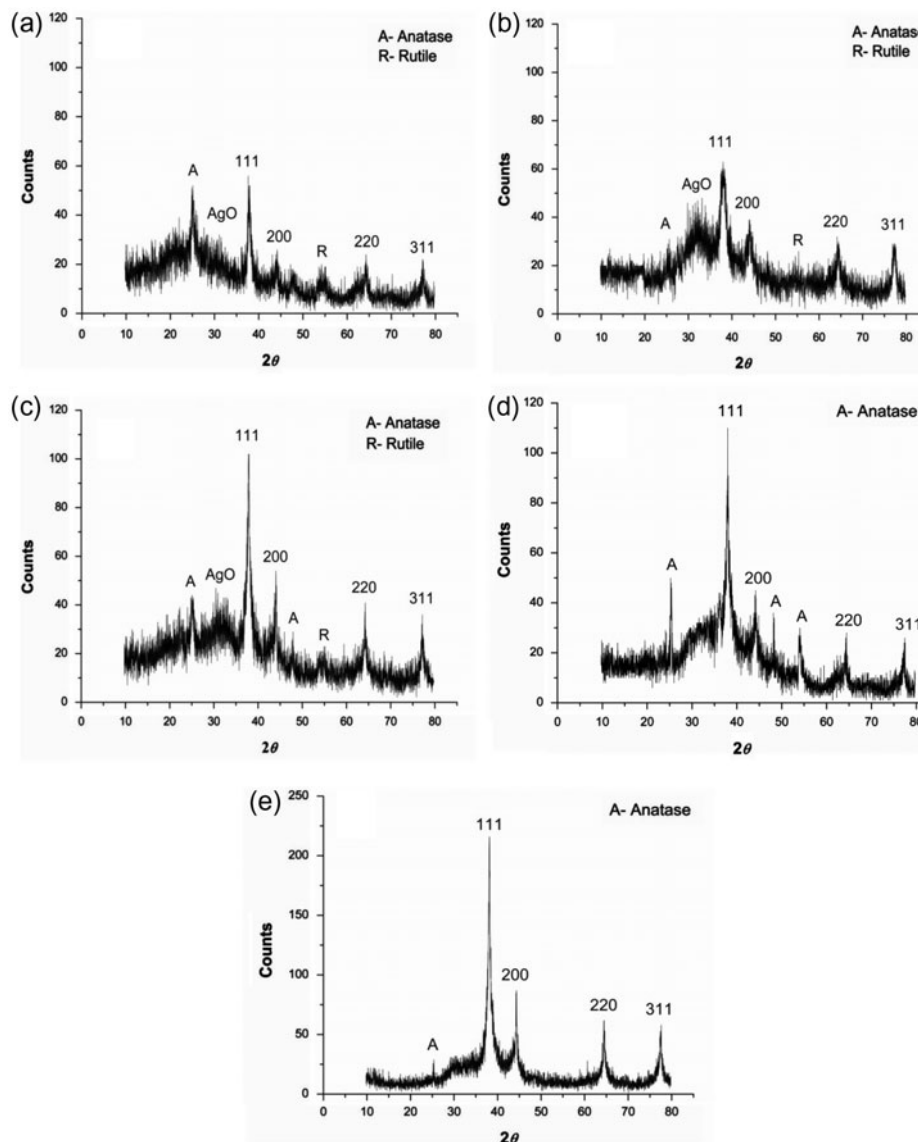


Fig. 8. X-ray diffractogram of Ag@TiO₂ synthesized with different Ag to Ti molar composition ratio and calcined at 450°C for 3 h. Ag to Ti molar ratio of (a) 1:5 mM, (b) 1:3.1 mM, (c) 1:2.2 mM, (d) 1:1.7 mM, and (e) 1:0.8 mM.

It can be observed that as the Ag to Ti molar ratio was increased from 1:5 to 1:1.7, the percentage degradation increased, but further increase in the ratio to 1:0.8 has lead to decrease in the degradation. The maximum degradation occurred with nanoparticles synthesized with Ag to Ti molar ratio of 1:1.7. In order to understand the reason for maximum photocatalytic activity by nanoparticles synthesized with 1:1.7 Ag to Ti ratio, XRD of the nanoparticles were obtained for all the nanoparticles synthesized with different Ag to Ti molar composition ratios (1:5, 1:3.1, 1:2.2, 1:1.7; 1:0.8) and calcined at 450°C for 3 h and are shown in Fig. 8(a)–(e).

Table 2 shows the presence of different crystal planes of Ag and TiO₂ in nanoparticles with different Ag to Ti molar composition ratio (1:5, 1:3.1, 1:2.2, 1:1.7; 1:0.8) at calcination temperature of 450°C with a calcination time of 3 h where (A) and (R) correspond to the anatase and rutile planes of TiO₂, respectively, and (111), (200), (220), and (311) correspond to the different crystal planes of Ag⁰. The XRD of nanoparticles with 1:1.7M composition ratio of Ag and Ti presented in Fig. 8(d) confirmed the crystalline nature of both core and shell. Formation of more of anatase phase was observed and crystallite size was found to be 39.40 nm [23].

Average crystallite size of Ag@TiO₂ nanoparticles prepared with different Ag to Ti molar composition ratio (1:5, 1:3.1, 1:2.2, 1:1.7; 1:0.8) was calculated based on the Scherrer's formula and are presented in Table 3. It was found from X-ray diffractogram of Ag@TiO₂

Table 3

Size of nanoparticles obtained with different Ag to Ti molar composition ratio at calcination temperature of 450°C for 3 h

Ag to Ti molar ratio	1:5	1:3.3	1:2.2	1:1.7	1:0.8
Crystallite size (nm)	68.70	60.11	56.61	39.40	27.46

catalysts of different compositions calcined at temperature of 450°C for 3 h shown in Fig. 8(a)–(e) and as summarized in Table 2 that as the Ag to Ti molar composition ratio was increased, increase in crystallinity was observed and it also resulted in increase in anatase phase of TiO₂. Decrease in particle size (Table 3) of Ag@TiO₂ nanoparticles was observed as the Ag to Ti molar composition ratio was increased from 1:5 to 1:0.8. Although smallest crystallite size was found with 1:0.8 Ag to Ti molar composition ratio as seen in Table 3, the X-ray diffractogram of Ag@TiO₂ presented in Fig. 8(e) showed only one anatase phase peak as compared to many anatase peaks in nanoparticles synthesized with 1:1.7 Ag to Ti molar composition ratio as shown in Fig. 8(d). In case of particles with 1:5, 1:3.1, 1:2.2 Ag to Ti molar composition ratios, both anatase and rutile phase formation were observed in XRD presented in Fig. 8(a)–(c) and peak for AgO was also found. Wang et al. [41] has reported that the presence of AgO in Ag@TiO₂ nanoparticles results in decrease in photocatalytic property. But in case of nanoparticles with 1:1.7M composition ratio (Fig. 8(d)), three peaks of anatase phase of TiO₂ and well-defined crystalline structure were found as com-

Table 2

Presence of different crystal planes of Ag and TiO₂ with different Ag to Ti molar composition ratio (1:5, 1:3.1, 1:2.2, 1:1.7; 1:0.8) at calcination temperature of 450°C with a calcination time of 3 h

Crystal planes of Ag and TiO₂ with different Ag to Ti molar ratio at calcination temperature of 450°C

Ag to Ti ratio	1:5 (Fig. 8(a))	1:3.1 (Fig. 8(b))	1:2.1 (Fig. 8(c))	1:1.7 (Fig. 8(d))	1:0.8 (Fig. 8(e))
Ag, 2θ (crystal plane)	37.63 (111) 44.13 (200) 64.30 (220) 77.21 (311)	37.90 (111) 44.11 (200) 64.20 (220) 77.40 (311)	37.90 (111) 44.11 (200) 64.14 (220) 77.14 (311)	37.94 (111) 44.20 (200) 64.30 (220) 77.10 (311)	37.98 (111) 44.38 (200) 64.50 (220) 77.50 (311)
TiO ₂ , 2θ (crystal plane)	25.10 (A) 55.13 (R)	25.72 (A) 55.17 (R)	25.10 (A) 48.01 (A)	25.30 (A) 48.14 (A) 54.02 (A)	25.50 (A)

Note: A: Anatase and R: Rutile.

pared to other compositions and no peaks of rutile TiO_2 and AgO were found. These are the main reasons of high photocatalytic activity shown by nanoparticles with 1:1.7M composition ratio. Highest photocatalytic activity with nanoparticles synthesized with Ag to Ti molar ratio of 1:1.7 can also be contributed to a Schottky energy barrier formed by the combination of Ag core and TiO_2 shells. The interface can attract light-induced electrons from the semiconductor TiO_2 to reduce electron-hole recombination. Presence of AgO resulted due to oxidation of Ag can be verified by the appearance of AgO diffraction peaks in Fig. 8(a)–(c) at lower Ag to Ti ratios. The AgO cannot serve as a Schottky energy barrier [41]. But no AgO peak was observed with nanoparticles synthesized with 1:1.7M ratio. Hence, lower photocatalytic activity was observed at Ag to Ti ratios of 1:5 to 1:2.2. From the results of photodegradation, the least Ag content sample (1:5) showed the least photocatalytic activity. This may also be because of the thicker TiO_2 shell which inhibits light-induced electrons from arriving at the interface between the Ag cores and the TiO_2 shells at low Ag to Ti ratio used during synthesis [41].

With 1:0.8 Ag to Ti molar composition ratio, in the XRD shown in Fig. 8(e), there was no AgO peak and though anatase phase peak was observed with low intensity. Ag (1,1,1) peak showed the highest intensity as compared to nanoparticles synthesized with other ratios, indicating that the silver content is predominant. So, lower photocatalytic activity shown by particles with 1:0.8 Ag to Ti molar composition ratio may be due to high Ag content and very less TiO_2 . Owing to high Ag and less Ti, not enough TiO_2 may be formed during the process to grow as a film around all the Ag nuclei. Surface coverage of Ag core with TiO_2 may be very less and the decreasing content of TiO_2 means that fewer electrons were generated to take part in the photodegradation of dyes, hence leading to lower photocatalytic activity.

Due to presence of more anatase phase, formation of well-defined crystalline structure with core-shell morphology and absence of AgO , Ag@TiO_2 nanoparticles synthesized with 1:1.7 Ag to Ti molar composition ratio, calcined at 450°C for 3 h was found to be the best in terms of photocatalytic activity.

Calcination time also affects the photocatalytic activity by determining the existence of crystalline phases. Fig. 9 shows the time course variation of percentage degradation of AB-129 dye during photocatalysis experiments carried out with Ag@TiO_2 nanoparticles prepared with 1:1.7 Ag to Ti molar composition ratio and calcined at 450°C for different calcination times.

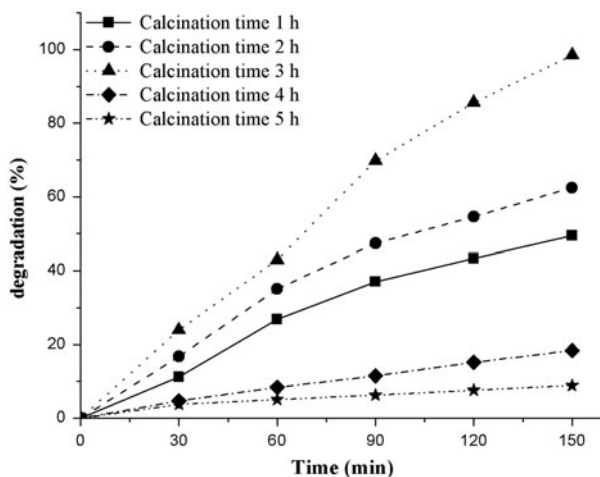


Fig. 9. Effect of calcination time on time course variation of solar photocatalytic degradation of AB-129 dye by Ag@TiO_2 . Ag to Ti molar ratio = 1:1.7; calcination temperature = 450°C ; pH 3, catalyst loading = 100 mg/L; $C_0 = 10$ mg/L; average UV and visible light intensity of solar light are 3.68 mW/cm^2 and $1,236 \times 10^2$ lux, respectively, from 11 am to 1.30 pm.

Time course variations have shown that the rate of degradation of the dye has increased with increase in calcinations time from 1 to 3 h, but further increase in calcinations time to 4 and 5 h has resulted in decreased rate of degradation. Effect of catalyst calcination time on percentage degradation of AB-129 dye (at 150 min irradiation time) with the catalyst calcined at different times is shown in Fig. 10.

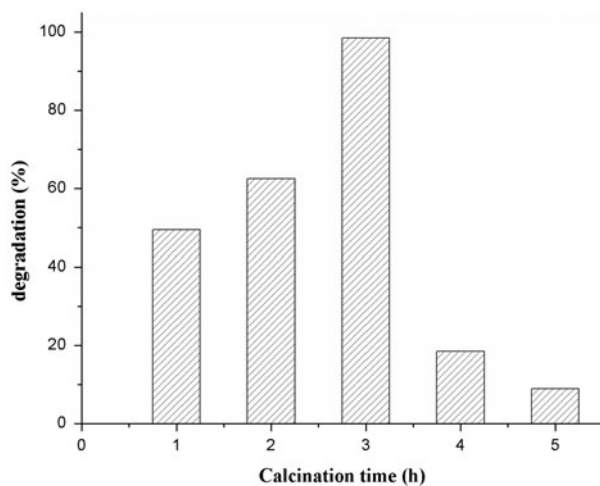


Fig. 10. Effect of calcination time on percentage degradation of AB-129 dye: pH 3; catalyst loading = 100 mg/L; $C_0 = 10$ mg/L; irradiation time = 150 min; average UV and visible light intensity of solar light are 3.68 mW/cm^2 and $1,236 \times 10^2$ lux, respectively, from 11 am to 1.30 pm.

It is observed that as the calcination time is increased from 1 to 3 h, the degradation in 150 min of irradiation time has increased from 49.5 to 98.5%, but further increase in calcination time to 4 and 5 h has decreased the degradation, which reached to only around 8.9% at 150 min irradiation time. Therefore, the highest degradation was observed at calcination time of 3 h. Increase in degradation of AB-129 may be attributed to increase in content of anatase in TiO_2 , which increases with increasing calcination time. It is reported by You et al. [42], Mozia et al. [43] and Wang et al. [36] that as calcination time increases, formation of anatase phase increase, but further increase in time leads to conversion of anatase phase to rutile phase which decreases the photocatalytic activity.

As seen from XRD (Fig. 8(d)) at calcination time of 3 h, anatase TiO_2 was found, so catalyst calcined at 450°C for 3 h showed better photocatalytic efficiency for photocatalytic degradation of AB-129 dye. As the calcination time increased, degradation increased, but further increase in the calcination time decreased the degradation. Therefore, calcination time of 3 h was found to be optimum.

Thus, the Ag@TiO_2 nanoparticles synthesized with Ag to Ti molar ratio of 1:1.7 and calcined at 450°C for 3 h were found to be optimum for maximum photocatalytic activity in terms of degradation of AB-129.

3.2. TEM image of Ag@TiO_2 core-shell nanoparticle

As Ag@TiO_2 nanoparticles synthesized with Ag to Ti molar ratio of 1:1.7 and calcined at 450°C for 3 h were found to be the optimum for maximum photo-

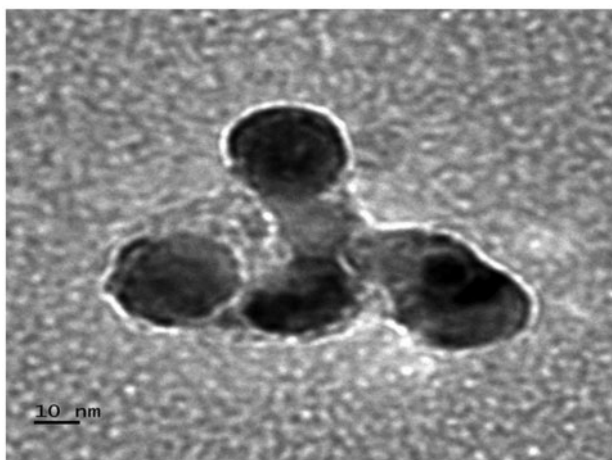


Fig. 11. TEM image of Ag@TiO_2 (Ag to Ti molar ratio of 1:1.7) nanoparticles calcined at 450°C for 3 h.

catalytic activity, these nanoparticles were analyzed using TEM. Fig. 11 illustrates TEM image of Ag@TiO_2 nanoparticles which confirmed the formation of core-shell structure with Ag core of approximate dimension of 33.63 nm and TiO_2 shell of average thickness 3.7 nm [23].

3.3. Comparison of solar photocatalytic activity of Ag@TiO_2 core-shell-structured nanoparticles with other photocatalysts for degradation of AB-129

For the photocatalysis of dyes, presently TiO_2 and Ag-doped TiO_2 are being used. So, solar photocatalytic activity of Ag@TiO_2 nanoparticles for degradation of AB-129 dye at initial concentration of 10 mg/L, pH of 3, and catalyst loading of 100 mg/L were compared with commercially available Degussa P-25 catalyst, TiO_2 (SG TiO_2), CST TiO_2 , Ag-doped-SG TiO_2 , Ag-doped (LI)-CST TiO_2 , and Ag-doped (PD)-CST TiO_2 . For Ag@TiO_2 and Ag-doped TiO_2 catalysts, Ag to Ti molar composition ratio of 1:1.7 was used. All synthesized TiO_2 and Ag-doped TiO_2 catalysts were calcined at 450°C for 3 h. Fig. 12 presents the time course variation of photocatalytic degradation of AB-129 by different catalyst.

The dissolved oxygen present in the reaction mixture acted as an oxidant in these experiments. In can be seen clearly that Ag@TiO_2 core-shell nanoparticles are more efficient in degradation of the dye as compared to Ag-doped TiO_2 and TiO_2 . As compared to

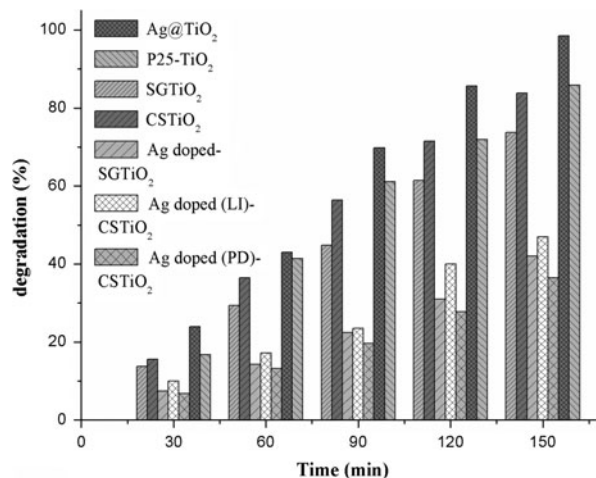


Fig. 12. Comparison of photocatalytic activity of different photocatalysts for solar photocatalysis of AB-129 dye: initial pH 3, catalyst loading = 100 mg/L, and $C_0 = 10$ mg/L, and average UV and visible light intensity of solar light are 3.72 mW/cm^2 and $1,240 \times 10^2$ lux, respectively, from 11 am to 1.30 pm.

the other photocatalysts, the degradation with Ag@TiO₂ nanoparticles is faster and around 98.5% degradation has been achieved in 150 min of irradiation. Photocatalytic activity in terms of degradation of AB-129 decreased in the order of Ag@TiO₂ > Degussa P-25 > SGTiO₂ > CSTiO₂ > Ag-doped (LI)-CSTiO₂ > Ag-doped-SGTiO₂ > Ag-doped (PD)-CSTiO₂. High photocatalytic efficiency is exhibited by Ag@TiO₂ which may be attributed to the inhibition of electron-hole recombination, by storage of electron in Ag core and subsequent discharge on provision of electron acceptor such as O₂ [11]. Lower photocatalytic activity shown by Ag-doped-SGTiO₂ and Ag-doped (LI)-CSTiO₂ may be due to the loss of activity of TiO₂ as metal deposits occupy the active sites on the TiO₂ surface [44]. Also least activity was shown by Ag-doped (PD)-CSTiO₂ as the negative charge on silver may start to attract holes and then recombine with electrons leading to recombination of electron hole [45], thus lower photocatalytic activity. Hence, it is concluded that Ag@TiO₂ nanoparticles synthesized by one-pot synthesis route with Ag to Ti molar ratio of 1:1.7 and calcined at 450°C for 3 h can be effectively used as a photocatalyst for the degradation of dyes by solar photocatalysis and the process may be effectively used in the treatment of dye/textile wastewater.

In order to study the extent of mineralization reached during solar photocatalysis of AB-129 dye with Ag@TiO₂ nanoparticles, TOC and COD analysis were carried out. Fig. 13 shows the time course varia-

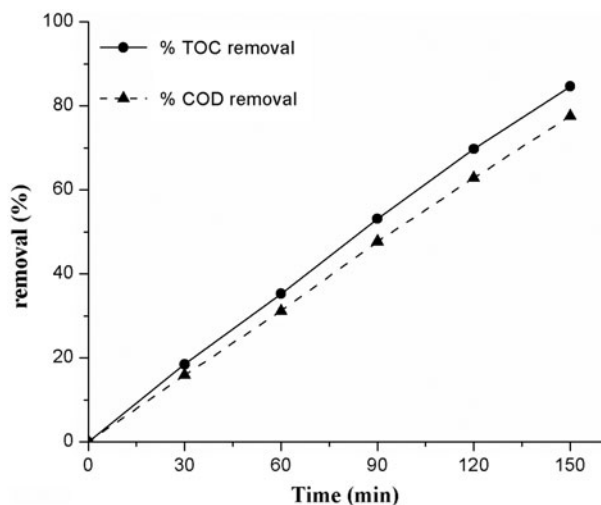


Fig. 13. Time course variation of percentage TOC and COD removal during solar photocatalysis of AB-129 dye: initial pH 3, catalyst loading = 100 mg/L, C₀ = 10 mg/L, and average UV and visible light intensity of solar light are 3.72 mW/cm² and 1,240 × 10⁻⁶ lux, respectively, from 11 am to 1.30 pm.

tion of percentage TOC and COD removal during solar photocatalysis of AB-129.

As shown in Fig. 13, percentage TOC removal and COD removal during photocatalysis of AB-129 have increased as the irradiation time is increased and around 85% TOC removal and around 78% COD removal occurred within 150 min of irradiation time. However, mineralization of AB-129 dye was not complete probably due to presence of intermediate compounds which were resistant to solar photocatalysis by the Ag@TiO₂ nanoparticles. Irradiation time may be further increased to cause further reduction in COD and TOC and hence to bring about further mineralization of the intermediates.

3.4. Kinetics of degradation of AB-129 by solar photocatalysis using Ag@TiO₂ nanoparticles

Study on kinetics helps in the designing of photocatalytic reactors for treatment of dye wastewater. Estimation of rate equation and parameters is an essential part of kinetics. So, kinetics of degradation of AB-129 with Ag@TiO₂ as the photocatalyst under solar light irradiation was studied at initial dye concentration of 10 mg/L, catalyst loading of 100 mg/L, and pH of 3. The results obtained during batch experiments were used for evaluation of kinetics. Langmuir-Hinshelwood (L-H) kinetic model (Eq. (2)) is widely used by various authors to describe solid-liquid reactions [21,46–50]. The effect of dye concentration on the rate of degradation is given in the form of (Eq. (2)) [51]:

$$r = \frac{kK_r[C]}{1 + K_r[C]} \quad (2)$$

where r is the rate of reaction of AB-129 dye, $[C]$ is the molar concentration of the dye at time t , k the constant related to adsorption, and K_r is the reaction rate constant. Eq. (2) is rewritten as Eq. (3):

$$\frac{1}{r} = \frac{1}{kK_r[C]} + \frac{1}{k} \quad (3)$$

To estimate the parameters in Eq. (3), rates of degradation were obtained by drawing tangents at different interval of time, on plots of dye concentration vs. time data obtained from the experiment. $1/r$ vs. $1/[C]$ was plotted and values for the kinetic parameters were estimated from the slope and intercept. Linear nature of the plot shown in Fig. 14 has validated the applicability of L-H equation.

The values of k and K_r are found to be 0.0003 mM min⁻¹ and 198.77 mM⁻¹ for degradation of AB-129 dye

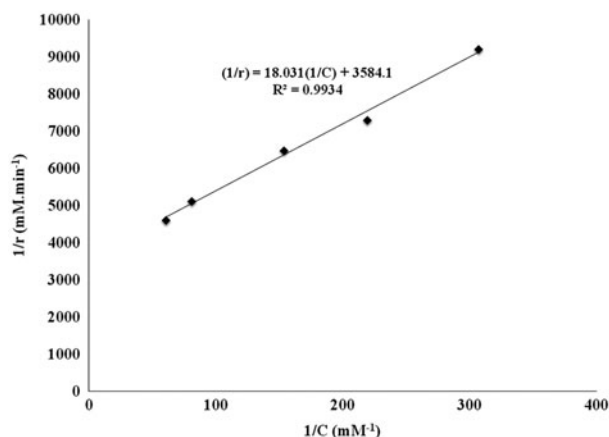


Fig. 14. Plot for L-H kinetics of solar photocatalysis of AB-129 dye using Ag@TiO₂ (Ag to Ti molar ratio of 1:1.7, calcined at 450°C for 3 h) as catalyst at conditions: pH 3; catalyst used = 100 mg/L.

degradation, respectively. This indicates that the degradation of dye occurred mainly on the surface of Ag@TiO₂ nanoparticles and the rate is proportional to the surface coverage of dye on the Ag@TiO₂ assuming that the dye is strongly adsorbed on the catalyst surface than the intermediate products [52].

4. Conclusions

Ag@TiO₂ nanoparticles were engineered by optimization of catalyst composition, calcination temperature, and calcinations time for enhanced solar photocatalytic activity to degrade AB-129 dye. The effect of these parameters on the solar photocatalytic activity of Ag@TiO₂ in terms of degradation of AB-129 dye was investigated. Ag to Ti molar composition ratio of 1:1.7, calcination temperature of 450°C, and calcinations time of 3 h are the most suitable conditions for synthesis and calcination of the photocatalyst and are considered the optimum. The X-ray diffractograms of Ag@TiO₂ showed the presence of both anatase and rutile forms of TiO₂ and Ag with different crystal plane, indicating the crystalline nature of core and the shell. It was found that Ag@TiO₂ nanoparticles showed highest catalytic efficiency for the degradation of AB-129 and photocatalytic activity is rated in the order of Ag@TiO₂ > Degussa P-25 > SGTiO₂ > CSTiO₂ > Ag-doped (LI)-CSTiO₂ > Ag-doped-SGTiO₂ > Ag-doped (PD)-CSTiO₂. Efficient mineralization can be achieved with Ag@TiO₂ nanoparticles. The photocatalytic degradation kinetics of AB-129 fitted well to the L-H model. Ag@TiO₂ core-shell-structured nanoparticles may be considered as effective catalysts for the solar photocatalytic degradation of AB-129 dye

and this process may be effectively used in the treatment of dye/textile wastewater.

Acknowledgment

The authors acknowledge the support provided by Department of Science and Technology, Government of India to carry out this research work.

References

- [1] C. Bauer, P. Jacques, A. Kalt, Photooxidation of an azo dye induced by visible light incident on the surface of TiO₂, *J. Photochem. Photobiol. A: Chem.* 140 (2001) 87–92.
- [2] S. Dai, Y. Zhuang, L. Chen, Study on the relationship between structure of synthetic organic chemicals and their biodegradability, *Environ. Chem.* 14 (1995) 354–367.
- [3] I. Šafařík, K. Nymburská, M. Šafaříková, Adsorption of water-soluble organic dyes on magnetic charcoal, *J. Chem. Technol. Biotechnol.* 69 (1997) 1–4.
- [4] I.K. Konstantinou, T.A. Albanis, TiO₂-assisted photocatalytic degradation of azo dyes in aqueous solution: Kinetic and mechanistic investigations, *Appl. Catal. B: Environ.* 49 (2004) 1–14.
- [5] S. Malato, J. Blanco, A. Vidal, C. Richter, Photocatalysis with solar energy at a pilot-plant scale: An overview, *Appl. Catal. B: Environ.* 37 (2002) 1–15.
- [6] M. Styliadi, D.I. Kondarides, X.E. Verykios, Pathways of solar light-induced photocatalytic degradation of azo dyes in aqueous TiO₂ suspensions, *Appl. Catal. B: Environ.* 40 (2003) 271–286.
- [7] C. Singh, R. Chaudhary, R.S. Thakur, Performance of advanced photocatalytic detoxification of municipal wastewater under solar radiation—A mini review, *Int. J. Energy Environ.* 2 (2011) 337–350.
- [8] M. Romero, J. Blanco, B. Sánchez, A. Vidal, S. Malato, A.I. Cardona, E. Garcia, Solar photocatalytic degradation of water and air pollutants: Challenges and perspectives, *Sol. Energy* 66(2) (1999) 169–182.
- [9] X.Z. Li, F.B. Li, Study of Au/Au³⁺-TiO₂ photocatalysts toward visible photooxidation for water and wastewater treatment, *Environ. Sci. Technol.* 35 (2001) 2381–2387.
- [10] X. You, F. Chen, J. Zhang, M. Anpo, A novel deposition precipitation method for preparation of Ag-loaded titanium dioxide, *Catal. Lett.* 102 (2005) 247–250.
- [11] T. Hirakawa, P.V. Kamat, Charge separation and catalytic activity of Ag@TiO₂ core-shell composite clusters under UV-irradiation, *J. Am. Chem. Soc.* 127 (2005) 3928–3934.
- [12] R.T. Tom, A.S. Nair, N. Singh, M. Aslam, C.L. Nandreda, R. Philip, K. Vijayamohan, T. Pradeep, Freely dispersible Au@TiO₂, Au@ZrO₂, Ag@TiO₂, and Ag@ZrO₂ core-shell nanoparticles: One-step synthesis, characterization, spectroscopy, and optical limiting properties, *Langmuir* 19 (2003) 3439–3445.
- [13] T. Ung, L.M. Liz-Marzán, P. Mulvaney, Controlled method for silica coating of silver colloids. Influence of coating on the rate of chemical reactions, *Langmuir* 14 (1998) 3740–3748.

- [14] I. Pastoriza-Santos, D.S. Koktysh, A.A. Mamedov, M. Giersig, N.A. Kotov, L.M. Liz-Marzán, One-pot synthesis of Ag@TiO₂ core-shell nanoparticles and their layer-by-layer assembly, *Langmuir* 16 (2000) 2731–2735.
- [15] S.C. Chan, M.A. Barteau, Preparation of highly uniform Ag/TiO₂ and Au/TiO₂ supported nanoparticle catalysts by photodeposition, *Langmuir* 21 (2005) 5588–5595.
- [16] T. Hirakawa, P.V. Kamat, Photoinduced electron storage and surface plasmon modulation in Ag@TiO₂ clusters, *Langmuir* 20 (2004) 5645–5647.
- [17] M. Abdulla-Al-Mamun, Y. Kusumoto, B. Ahmmad, M. Shariful Islam, Photocatalytic cancer (HeLa) cell-killing enhanced with Cu-TiO₂ nanocomposite, *Top. Catal.* 53 (2010) 571–577.
- [18] A.V. Rupa, D. Divakar, T. Sivakumar, Titania and noble metals deposited titania catalysts in the photodegradation of tartazine, *Catal. Lett.* 132 (2009) 259–267.
- [19] K. Nagaveni, G. Sivalingam, M.S. Hegde, G. Madras, Solar photocatalytic degradation of dyes: High activity of combustion synthesized nano TiO₂, *Appl. Catal. B: Environ.* 48 (2004) 83–93.
- [20] L.C. Zhang, K.F. Cai, X. Yao, Preparation, characterization and photocatalytic performance of Co/Ni Co-doped TiO₂ nanopowders, *J. Electroceram.* 21 (2008) 512–515.
- [21] C. Sahoo, A.K. Gupta, A. Pal, Photocatalytic degradation of Crystal Violet (C.I. Basic Violet 3) on silver ion doped TiO₂, *Dyes Pigm.* 66 (2005) 189–196.
- [22] M.A. Behnajady, N. Modirshahla, M. Shokri, B. Rad, Enhancement of photocatalytic activity of TiO₂ nanoparticles by silver doping: Photodeposition versus liquid impregnation methods, *Global Nest J.* 10 (2008) 1–7.
- [23] A. Khanna, V.K. Shetty, Solar photocatalysis for treatment of Acid Yellow-17 (AY-17) dye contaminated water using Ag@TiO₂ core-shell structured nanoparticles, *Environ. Sci. Pollut. Res.* 20 (2013) 5692–5707.
- [24] APHA, Standard Methods for Water and Wastewater Examination, 19th ed., APHA, Washington, DC, 1995.
- [25] S. Angkaew, P. Limsuwan, Preparation of silver-titanium dioxide core-shell (Ag@TiO₂) nanoparticles: Effect of Ti-Ag mole ratio, *Procedia Eng.* 32 (2012) 649–655.
- [26] M. Sathish, B. Viswanathan, R.P. Viswanath, Characterization and photocatalytic activity of N-doped TiO₂ prepared by thermal decomposition of Ti-melamine complex, *Appl. Catal. B: Environ.* 74 (2007) 307–312.
- [27] D. Li, H. Haneda, S. Hishita, N. Ohashi, Visible-light-driven nitrogen-doped TiO₂ photocatalysts: Effect of nitrogen precursors on their photocatalysis for decomposition of gas-phase organic pollutants, *Mater. Sci. Eng. B* 117 (2005) 67–75.
- [28] J. Ovenstone, Synthesis of TiO₂ by sol-gel methods, *J. Mater. Sci.* 36 (2001) 1325–1329.
- [29] J.G. Yu, H.G. Yu, B. Cheng, X.J. Zhao, J.C. Yu, W.K. Ho, The effect of calcination temperature on the surface microstructure and photocatalytic activity of TiO₂ thin films prepared by liquid phase deposition, *J. Phys. Chem. B* 107 (2003) 13871–13879.
- [30] H.G. Yu, J.G. Yu, B. Cheng, J. Lin, Synthesis, characterization and photocatalytic activity of mesoporous titania nanorod/titanate nanotube composites, *J. Hazard. Mater.* 147 (2007) 581–587.
- [31] J.G. Yu, J.F. Xiong, B. Cheng, S.W. Liu, Fabrication and characterization of Ag-TiO₂ multiphase nanocomposite thin films with enhanced photocatalytic activity, *Appl. Catal., B: Environ.* 60 (2005) 211–221.
- [32] M. Mrowetz, W. Balcerski, A.J. Colussi, M.R. Hoffmann, Oxidative power of nitrogen-doped TiO₂ photocatalysts under visible illumination, *J. Phys. Chem. B* 108 (2004) 17269–17273.
- [33] K.Y. Jung, S.B. Park, Effect of calcination temperature and addition of silica, zirconia, alumina on the photocatalytic activity of titania, *Korean J. Chem. Eng.* 18 (2001) 879–888.
- [34] L. Jing, Y. Qu, B. Wang, S. Li, B. Jiang, L. Yang, W. Fu, H. Fu, Review of photoluminescence performance of nano-sized semiconductor materials and its relationships with photocatalytic activity, *Sol. Energy Mater. Sol. Cells* 90 (2006) 1773–1787.
- [35] R.I. Bickley, T.J. Gonzalez-carreno, J.S. Lees, A structural investigation of titanium dioxide photocatalysts, *J. Solid State Chem.* 92 (1991) 178–190.
- [36] J. Wang, J. Li, Y. Xie, C. Li, G. Han, L. Zhang, R. Xu, X. Zhang, Investigation on solar photocatalytic degradation of various dyes in the presence of Er³⁺: YAlO₃/ZnO-TiO₂ composite, *J. Environ. Manage.* 91 (2010) 677–684.
- [37] J. Ovenstone, K. Yanagisawa, Effect of hydrothermal treatment of amorphous titania on the phase change from anatase to rutile during calcination, *Chem. Mater.* 11 (1999) 2770–2774.
- [38] D. Zhang, X. Song, R. Zhang, M. Zhang, F. Liu, Preparation and characterization of Ag@TiO₂ core-shell nanoparticles in water-in-oil emulsions, *Eur. J. Inorg. Chem.* 2005 (2005) 1643–1648.
- [39] G. Sivalingam, K. Nagaveni, M.S. Hegde, G. Madras, Photocatalytic degradation of various dyes by combustion synthesized nano anatase TiO₂, *Appl. Catal. B: Environ.* 45 (2003) 23–38.
- [40] T. Aarthi, P. Narahari, G. Madras, Photocatalytic degradation of Azure and Sudan dyes using nano TiO₂, *J. Hazard. Mater.* 149 (2007) 725–734.
- [41] W. Wang, J. Zhang, F. Chen, D. He, M. Anpo, Preparation and photocatalytic properties of Fe³⁺-doped Ag@TiO₂ core-shell nanoparticles, *J. Colloid Interface Sci.* 323 (2008) 182–186.
- [42] X. You, F. Chen, J. Zhang, Effects of calcination on the physical and photocatalytic properties of TiO₂ powders prepared by sol-gel template method, *J. Sol-Gel Sci. Technol.* 34 (2005) 181–187.
- [43] S. Mozia, Effect of calcination temperature on photocatalytic activity of TiO₂. Photodecomposition of mono- and polyazo dyes in water, *Pol. J. Chem. Technol.* 10 (2008) 42–49.
- [44] O. Carp, C.L. Huisman, A. Reller, Photoinduced reactivity of titanium dioxide, *Prog. Solid State Chem.* 32 (2004) 33–177.
- [45] H.M. Coleman, K. Chiang, R. Amal, Effects of Ag and Pt on photocatalytic degradation of endocrine disrupting chemicals in water, *Chem. Eng. J.* 113 (2005) 65–72.
- [46] W.Z. Tang, H. An, UV/TiO₂ photocatalytic oxidation of commercial dyes in aqueous solutions, *Chemosphere* 31 (1995) 4157–4170.

- [47] C. Galindo, P. Jacques, A. Kalt, Photooxidation of the phenylazonaphthol AO20 on TiO₂: Kinetic and mechanistic investigations, *Chemosphere* 45 (2001) 997–1005.
- [48] M. Muruganandham, M. Swaminathan, Solar photocatalytic degradation of a reactive azo dye in TiO₂-suspension, *Sol. Energy Mater. Sol. Cells* 81 (2004) 439–457.
- [49] N. Daneshvar, M.H. Rasoulifard, A.R. Khataee, F. Hosseinzadeh, Removal of C.I. Acid Orange 7 from aqueous solution by UV irradiation in the presence of ZnO nanopowder, *J. Hazard. Mater.* 143 (2007) 95–101.
- [50] G. Zayani, L. Bousselmi, F. Mhenni, A. Ghrabi, Solar photocatalytic degradation of commercial textile azo dyes: Performance of pilot plant scale thin film fixed-bed reactor, *Desalination* 248 (2009) 23–31.
- [51] R.W. Matthews, Photooxidation of organic impurities in water using thin films of titanium dioxide, *J. Phys. Chem.* 91 (1987) 3328–3333.
- [52] H. Al-Ekabi, N. Serpone, Kinetics studies in heterogeneous photocatalysis. I. Photocatalytic degradation of chlorinated phenols in aerated aqueous solutions over titania supported on a glass matrix, *J. Phys. Chem.* 92 (1988) 5726–5731.